Carbohydrate Polymers 92 (2013) 934–941

Contents lists available at SciVerse ScienceDirect

Carbohydrate Polymers

journal homepage: www.elsevier.com/locate/carbpol

Study of *Astragalus mongholicus* polysaccharides on endothelial cells permeability induced by HMGB1

Yun-Jiang Zheng[a,1], Bin Zhou[a,1], Zhi-Fang Song[a], Lei Li[b], Jun Wu[b], Ru-Yuan Zhang[b], Yao-Qing Tang[b,*]

[a] *Emergency Department, Chongming Branch, Xin Hua Hospital, Shanghai Jiao Tong University School of Medicine, Shanghai 202150, China*
[b] *Surgical Intensive Care Units, Rui Jin Hospital, Shanghai Jiao Tong University School of Medicine, Shanghai 200025, China*

ARTICLE INFO

Article history:
Received 20 September 2011
Received in revised form 28 July 2012
Accepted 1 August 2012
Available online 12 September 2012

Keywords:
Astragalus mongholicus polysaccharide
Endothelial permeability
High mobility group protein 1
Rho/ROCK

ABSTRACT

Astragalus mongholicus polysaccharide (APS) shows various biological activities. Here, we explored the effect of APS on high mobility group protein 1 (HMGB1) -induced endothelial cell permeability. The results indicated APS pretreatment effectively inhibited HMGB1-induced increased permeability in endothelial cells (ECs). Signal transduction studies showed APS inhibited not only the activation of small guanylate Rho and its downstream effector Rho kinase (ROCK), but also the subsequent phosphorylation of myosin light chain (MLC) in ECs. In conclusion, our investigations suggested that APS inhibited HMGB1-induced increased permeability in ECs, regulated by Rho/ROCK signal pathways.

1. Introduction

Endothelial cells (ECs) line blood vessels and form a physical barrier that separates the vascular lumen from the surrounding tissues. ECs control the passage of solutes, macromolecules, and cells from the blood into the tissues, a role particularly important for immune and inflammatory responses. However, ECs loss the integrity of the barrier function and increased permeability, when attacked by inflammatory cytokines such as tumor necrosis factor (TNF-α) and endotoxin. Then, some macromolecules, like proteins, inflammatory mediators, which usually cannot be passed through, permeate from the vascular lumen to the surrounding tissue to cause the symptoms of capillary leak syndrome (CLS), including local tissue edema, hypovolemic shock, organ dysfunction, etc. (Downie, Ryan, Hayes, & Friedman, 1992; Liu et al., 2005; Yong et al., 2010). Studies have shown that, endothelial cell cytoskeleton proteins and endothelial cell junction proteins constitute a main permeability barrier. Endothelial cell cytoskeleton, especially filamentous actin (F-acting) reorganization and redistribution, are main pathological basis in increased endothelial permeability, which cause the increase in cell contraction and intercellular gap formation (Cines et al., 1998; Shivanna, Rajashekhar, & Srinivas, 2010). It is reported that the changes of endothelial cytoskeletal morphology are mainly regulated by small nucleotide Rho and its downstream effector Rho kinase (ROCK) (van Nieuw Amerongen et al., 2007). The activation of ROCK causes phosphorylation of type II myosin light chain (MLC) and increases actomyosin interaction in ECs.

High mobility group protein 1 (HMGB1), as a fatal inflammatory mediator, is released in late endotoxemia (Wang et al., 1999). The levels of HMGB1 in serum are positive correlation with mortality of patients with sepsis (Bitto et al., 2010; Karlsson et al., 2008). HMGB1 can induce the activation of microvascular ECs, increase the expression of adhesion molecules, inflammatory cytokines and enhance plasmin activity, by its combination with membrane receptors for advanced glycation end products receptor (RAGE) expressed in ECs membrane (Fiuza et al., 2003). It is reported that HMGB1 could induce human pulmonary artery endothelial cell barrier dysfunction (Wolfson, Chiang, & Garcia, 2011). Due to its long duration in plasma, HMGB1 has obviously kinetic characteristics, which differ from the early classical pro-inflammatory cytokines such as TNF-α and IL-1β. Therefore, it can provide a wide therapeutic window for interfering with CLS (Huston et al., 2007).

Astragalus mongholicus polysaccharide (APS) is the main ingredient of Astragali Radix. Studies have revealed the anti-inflammatory, antioxidant, and immune regulatory roles of APS (Liu, Yao, Yu, Dong, & Sheng, 2011; Liu, Yao, Zhang, & Sheng, 2011; Shao, Zhao, Zhi-Chen, & Pan, 2006). Lee et al. reported that Astragali Radix appeared to exert immune modulating effects by regulating the expression of cytokines, such as interleukin (IL)-1, IL-6 and inducible nitric oxide synthase (iNOS), as well as the production of nitric oxide (NO) (Lee et al., 2005). Study showed that APS exerted its anti-inflammatory effects by blocking mitogen

* Corresponding author.
E-mail addresses: zyjgyh@hotmail.com (Y.-J. Zheng), yaoqt@medmail.com.cn (Y.-Q. Tang).
[1] These authors contributed to this work equally.

0144-8617/$ – see front matter © 2012 Elsevier Ltd. All rights reserved.
http://dx.doi.org/10.1016/j.carbpol.2012.08.001

activated protein kinase (MAPK) transcriptional activity to inhibit lipopolysaccharide-induced production of TNF-α and interleukin-8 in intestinal epithelial cells (Yuan, Sun, & Li, 2009). However, the knowledge of how APS exerts its protecting endothelial barrier dysfunction induced by pro-inflammatory cytokines is still limited. In this study, the effects of APS on HMGB1-induced Rho/ROCK signaling pathway and endothelial permeability in human umbilical vein endothelial cells (HUVECs) in vitro were investigated, showing that APS prevented the activation of Rho/ROCK signaling pathway and inhibited a significant increase in ECs permeability.

2. Materials and methods

2.1. Chemicals and regents

APS was purchased from the Chinese Medicinal Herbs Company (Beijing, China), with a purity of 95% and each 250 mg. EA.hy926 endothelial cell line was a gift from Dr. Cora-Jean S. Edgell and isolated from human embryonic umbilical vein endothelial cells. MLC, FITC-conjugated goat anti-mouse and rabbit secondary antibodies, Y-27632, C3-transferase and TRITC–phalloidin were from Sigma–Aldrich, p-MLC (Thr18), ZO-1 antibodies were from Santa Cruz Biotechnology, RhoA antibody from BD Transduction Laboratories, Rho activation kit from Upstate Biotechnology (Millipore), HMGB1 from Proteintech, factor VIII-related antibody from Shrek (Shanghai).

2.2. Extraction and purification of APS

Samples (500 g) were dried at 80 °C then crushed. 8 volumes of water were added to the samples, boiled for 2 h followed by filtering. Residues were then dissolved in 6 volumes of water, boiled for 1 h, filtered, reconstituted again with 4 volumes of water, boiled for 0.5 h, and then filtered. The three filtrates were combined then concentrated. A yield of tan crude APS was obtained after deproteinization using the Savage method and precipitation, centrifugation and evaporation. Sephadex G-150 column chromatography was then performed: 1 g crude APS was dissolved in 0.1 mol/l NaCl solution and was added to the chromatography column, then eluted by 0.1 mol/l NaCl solution with a maintained flow rate of 0.5 ml/min. Every pipe detection (2 ml per tube) was performed using the sulfuric acid–phenol method, then combined with a single peak and freeze-dried. Thus, the Boutique of APS were obtained.

2.3. Structure and composition of APS

Determination of monosaccharide composition of APS: polysaccharide samples (5 mg) were mixed with 2 ml sulfuric acid (1 mol/l) solution in an ampule and then sealed. Then, the compound was hydrolyzed in boiling water for 8 h, cooled, neutralized by $BaCO_3$, and then filtered. The supernatant was lyophilized then dissolved by adding 2 ml pyridine. Derivatization was performed by quickly adding 0.6 ml trimethylchlorosilane and 0.4 ml hexamethyldisilane at room temperature for 15 min. Derivatives (1 μl) were analyzed by gas chromatography. The gas chromatographic conditions were as follows: column DB-5 2 m long, 3 mm i.d.; fixative: 10% SE-30; gas flow rate: carrier gas N_2: 20 ml/min, H_2: 16 ml/min, air: 150 ml/min; column temperature: 195 °C; detector temperature: 230 °C; vaporizer temperature: 230 °C. Infrared spectrum analysis of the APS was carried out using a spectrum 100-Fourier transform infrared spectrometer (FT-IR) (PerkinElmer, USA): the operating range was from 4400 to 450 cm^{-1} with a resolution of 4 cm^{-1} using a DTGS detector. Following pellet preparation, polysaccharide samples (2 mg) were mixed with dry KBr (400 mg), and grinded in an agate mortar for 10 min. KBr pellets were immediately placed into the sample compartment of the spectrometer, and FT-IR spectra were subsequently recorded.

2.4. Cell culture

ECs were cultured in DMEM medium supplemented with 10% fetal bovine serum (FBS), 150 units/ml penicillin and 150 units/ml streptomycin at 37 °C under 5% CO_2 and 95% air. Cell morphology was observed under the microscope and identified by factor VIII immunofluorescence staining. When growing to sub-confluence, cells were pretreated with vehicle or various concentrations of APS (50–500 μg/ml) in DMEM with 10% FBS for indicated time. The culture medium was removed as followed by washing twice with phosphate buffered saline (PBS, PH 7.4), and then the cells were exposed to various concentrations of HMGB1 (50–1000 ng/ml) diluted in culture medium for different time intervals at 37 °C until further analysis. Cell viability was determined by trypan blue exclusion under all experimental conditions.

2.5. Determination of cell permeability

ECs were grown on 3-μm pore Transwell filters (Corning Costar Corporation, USA) until confluent and transferred into starvation medium containing 1% FBS for 2 h. FITC-dextran (MR 42,000; Sigma–Aldrich) was applied apically at 1 μg/ml and allowed to equilibrate for 30 min before a sample of the medium was removed from the lower chamber to measure basal permeability. Monolayers were pre-treated with APS (50–500 μg/ml) for 24 h and then either left untreated (control), or stimulated in triplicate with HMGB1 (50–1000 ng/ml), samples were taken from the lower chamber for fluorescence measurements and compared to the control monolayers. Where Y-27632 or C3 transferase were used, the inhibitors were added for the final 4 h of the 24 h HMGB1 incubation and FITC–dextran was applied after 24 h of HMGB1 stimulation. A sample of the medium was taken from the lower chamber 1 h subsequent to this. The fluorescence intensity of FITC was detected using a fluorescence spectrometer (LS-50B, PE Company, USA), excitation wavelength 492 nm; detection wavelength 520 nm.

2.6. Immunofluorescence staining and confocal microscopy

For F-actin staining, ECs were fixed for 10 min in 3.7% formaldehyde at 4 °C. Cells were permeabilized in 0.2% Triton-X-100 for 5 min. And then the cells were blocked in 1% bovine serum albumin (BSA) in PBS, and incubated with TRITC–phalloidin (2 kU/L) at room temperature away from light for 1 h. For ZO-1 staining, ECs were fixed for 10 min in 3.7% formaldehyde at 4 °C. Cells were then blocked in 1% bovine serum albumin (BSA) in PBS, and incubated sequentially with mouse anti-ZO-1 protein antibody (1:100) overnight at room temperature, and then FITC-labeled goat anti-mouse IgG secondary antibody (1:200) at room temperature away from light incubated for 1 h. Images were collected using a confocal laser scanning microscope (LSM410, Zeiss, Germany).

2.7. Rho pull-down assays

Rho pull-down assays were carried out as previously described (Ren and Schwartz, 2000). Glutathione sepharose-coupled GST-RBD (Rhotekin Rho-binding domain) beads (20 mg per pull-down) were used (Upstate Biotechnology). ECs were starved for 2 h and pre-treated with APS (200 and 500 μg/ml) for 24 h and either left unstimulated, or stimulated with 1000 ng/ml HMGB1 for 30 min prior to rapid lysis in pull-down lysis buffer (50 mM Tris pH 7.5, 1% Triton-X-100, 0.5% sodium deoxycholate, 0.1% SDS, 500 mM NaCl, 100 mM $MgCl_2$, 10 mg/ml leupeptin, 10 mg/ml aprotonin, 1 mM PMSF, 10% glycerol, 1 mM DTT). Cells were scraped immediately,

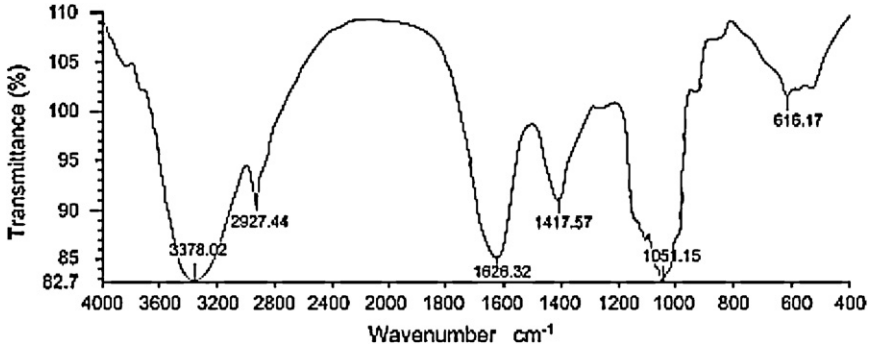

Fig. 1. FT-IR analysis of *Astragalus mongholicus* polysaccharide.

transferred into a microfuge tube and centrifuged at 13,000 × *g* for 3 min at 4 °C. A 50 ml sample of the whole cell lysate was retained, and the remaining supernatant was incubated with the GST-RBD beads at 4 °C with rotation for 1 h. The beads were washed three times in pull-down lysis buffer, boiled for 5 min in Laemmli sample buffer. Proteins were then resolved by SDS-PAGE and Western blotted. Protein concentration in the whole cell lysates was determined by a BioRad assay. Protein loading on the gel was determined by reprobing the whole cell lysate lanes with an anti-GAPDH antibody.

2.8. Cell lysate

For isolation of total cell extracts, the ECs were lysed in 200 μl of cell lysis buffer (20 mM Tris–HCl with pH 7.5, 150 mM NaCl, 1 mM Na_2EDTA, 1 mM EGTA, 1% Triton, 2.5 mM sodium pyrophosphate, 1 mM β-glycerophosphate, 1 mM Na_3VO_4, 1 μg/ml aprotonin and 1 μg/ml leupeptin), to which 1 mM PMSF was added before use. Concentration of protein samples was determined with the use of BioRad Protein Assay kit (BioRad Protein Assay, USA) and all samples were kept at −80 °C until further analysis.

2.9. Western blotting analysis

ECs were lysed with a SDS sample buffer. The supernatants were analyzed by 10% SDS-PAGE. Proteins were transferred to nitrocellulose membranes, which were blocked with 10% nonfat dry milk in TBST containing 20 mmol/L Tris (pH 8.0), 137 mmol/L NaCl and 10% Tween-20, and blotted with the relevant primary antibody, then with a horseradish peroxidase-conjugated secondary antibody. Bound proteins were detected by enhanced chemiluminescence according to its manufacturer's instructions.

2.10. Statistical analysis

Statistical analysis was performed using SPSS 10.0 package. Data were expressed as mean ± SE. Statistical significance of differences among values was determined by ANOVA and LSD was used for inter-group comparison. $p < 0.05$ was considered statistically significant.

3. Results and discussions

3.1. Monosaccharide composition and purity of APS

The yield of APS was 32% of the plant raw material and the purity was 95% as judged by using the sulfuric acid–phenol method. The results of gas chromatographic quantitative analysis of the derivatives of monosaccharides revealed a composition of glucose, mannose, galactose and fructose, and trace amounts of fucose and xylose. The molar ratio was as follows: 22.776:3.518:1:3.704:2.981:0.745, respectively (Table 1). This showed that the APS was a glucose-based hybrid polysaccharide.

Table 1
Molar ratio of the monosaccharides found in *Astragalus mongholicus* polysaccharide.

Glucose	Galactose	Mannose	Fructose	Fucose	Xylose
22.776	1	3.518	3.704	2.981	0.745

In Fig. 1, the infrared spectrum of APS was typical of polysaccharides, where peak absorptions were found at 3378.02, 2927.44, 1626.32, 1417.57, 1051.15 and 616.17 cm^{-1}. The broad absorption peak in the region of 3378.02 cm^{-1} corresponded to O—H bond stretching vibration, which indicated that the polysaccharide contained intermolecular and intramolecular hydrogen bonds. The band in the region of 2927.44 cm^{-1} corresponding to saturated C—H stretching vibration combined with the band in the region of 1417.57 cm^{-1} corresponding to C—H bending vibration reflected the characteristic absorption spectra of carbohydrates. The band in the region of 1626.32 cm^{-1} was the polysaccharide hydration absorption peak. The absorption peak from 1200 to 1000 cm^{-1} was due to C—O stretching vibration located in the sugar rings and glycosidic bonds.

3.2. Identification of EA.hy926 endothelial cell line

Under a microscope, morphological changes of ECs are from round to gradually becoming spindle-shaped, oval. Factor VIII immunofluorescence staining is positive (Fig. 2).

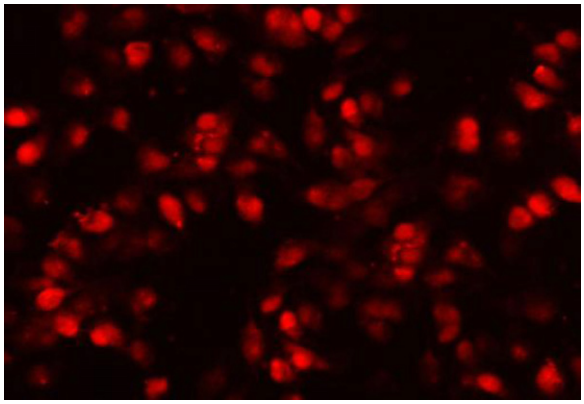

Fig. 2. EA.hy926 endothelial cell factor VIII immunofluorescence staining. *Note*: VIII factor staining > 95%.

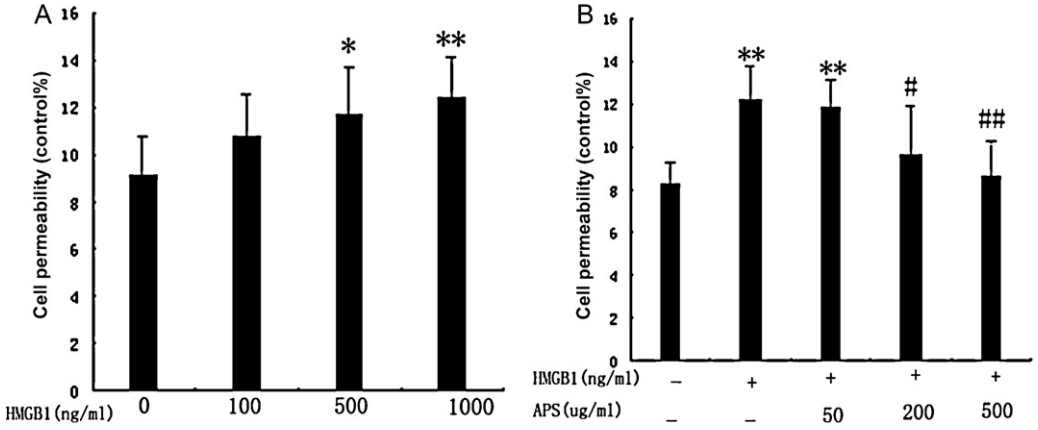

Fig. 3. Inhibitory effects of APS pretreatment on increased permeability of ECs induced by HMGB1. (A) Cells were exposed to HMGB1 (100–1000 ng/ml) for 12 h. (B) Cells were pretreated with APS (50–500 μg/ml) for 24 h before exposure to HMGB1 (1000 ng/ml) for 12 h. Data are presented as means ± SD ($n = 6$). $^{*}p < 0.05$ and $^{**}p < 0.01$ compared to the control group; $^{\#}p < 0.05$ and $^{\#\#}p < 0.01$ compared to the HMGB1-treated group.

3.3. Inhibition of APS pretreatment on cell permeability of HMGB1-induced in ECs

The effect of APS pretreatment on cell permeability of HMGB1-induced in ECs was evaluated by immunofluorescence assay. AS shown in Fig. 3A, HMGB1 treatment (50–1000 ng/ml) for 12 h obviously increased the cell permeability in a concentration-dependent manner, especially when using HMGB1 1000 ng/ml, showing significantly different ($p < 0.01$, compared with the control groups), which was reversed by APS pretreatment (200 and 500 μg/ml) for 24 h (Fig. 3B). Of which, APS (500 μg/ml) pretreatment had a very significant difference (compared with the HMGB1-treated groups, $p < 0.01$). It should be noted that APS itself had no significant effect on ECs permeability ($p > 0.05$).

3.4. Effects of APS pretreatment on HMGB1-induced morphology of endothelial cytoskeleton actin

Endothelial permeability barrier is mainly comprised of the skeleton and junction proteins of ECs (Xiaolu et al., 2011). Endothelial cell cytoskeleton, especially filamentous actin (F-actin) reorganization and redistribution, are main pathological basis in

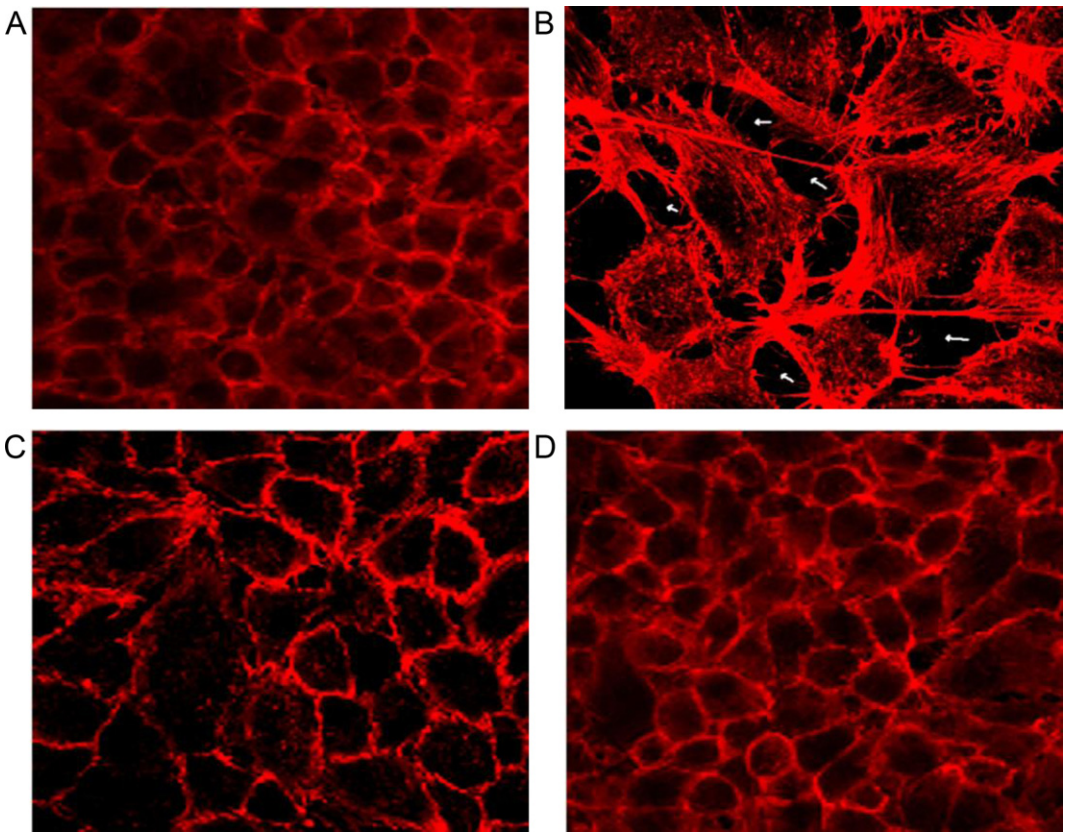

Fig. 4. Effect of APS pretreatment on HMGB1-induced morphological change of endothelial cytoskeleton actin. ECs were treated with APS for 24 h, and cultured in a medium containing 1000 ng/ml HMGB1 for 12 h to detect morphology of endothelial cytoskeleton F-actin by confocal microscope. (A) Control group; (B) HMGB1 + 0 μg/ml APS group; (C) HMGB1 + 200 μg/ml APS group; (D) HMGB1 + 500 μg/ml APS group; arrow indicates gap, bars = 20 μm.

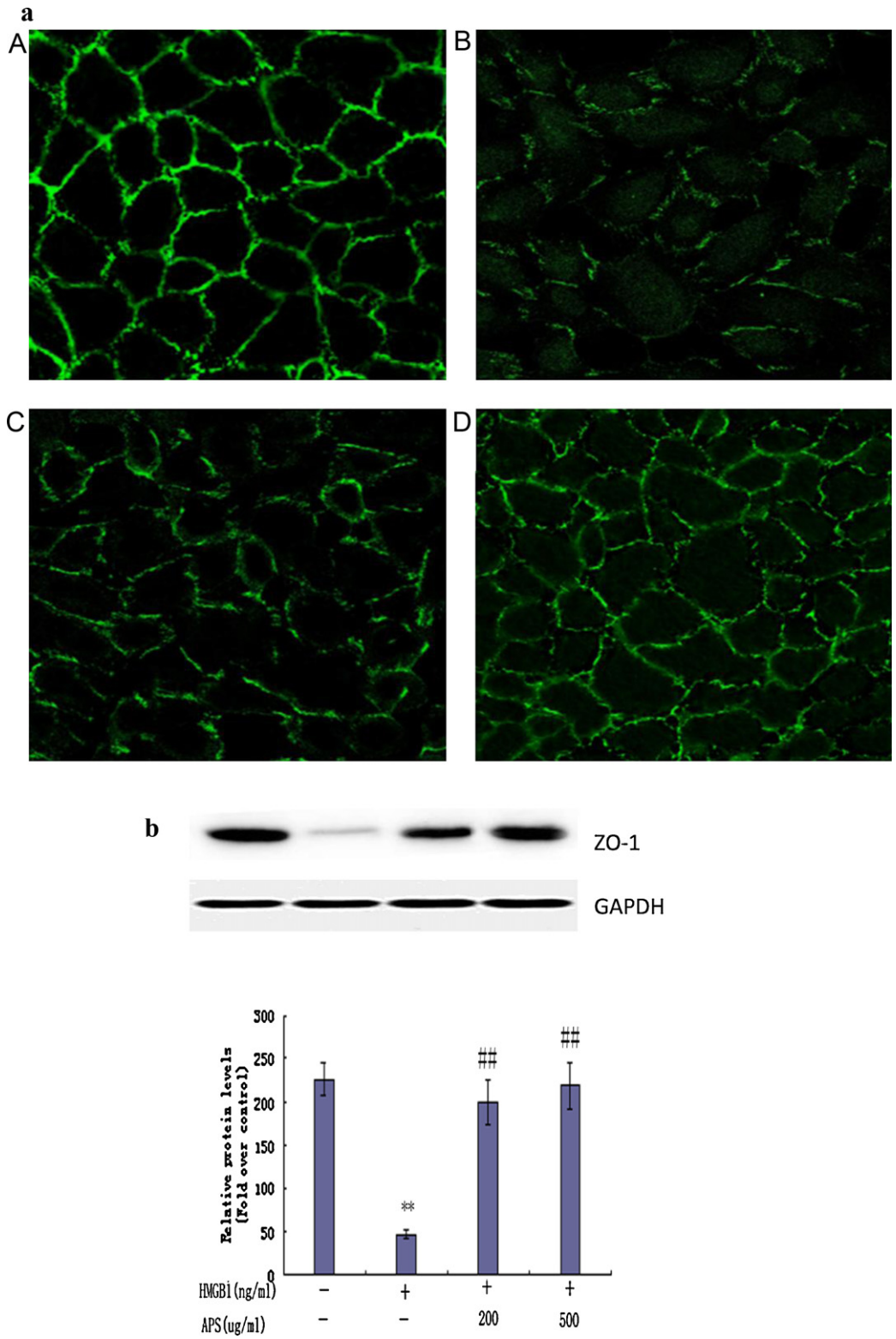

Fig. 5. (a and b) Inhibitive effects of APS on HMGB1-induced ZO-1 morphological changes of endothelial tight junction protein ZO-1 and its protein expressions in ECs. Cells were pretreated with APS for 24 h and then exposed to HMGB1 (1000 ng/ml) for 12 h. (A) Control group; (B) HMGB1 + 0 μg/ml APS group; (C) HMGB1 + 200 μg/ml APS group; (D) HMGB1 + 500 μg/ml APS group. Bars = 20 μm. Data were represented as mean ± SD ($n = 6$). $^{**}p < 0.01$ compared to the control group; $^{\#\#}p < 0.01$ compared to the HMGB1-treated group.

increased endothelial permeability, which caused the increase in cell contraction and intercellular gap formation (Cines et al., 1998; Shivanna et al., 2010). In this study, prior to HMGB1 stimulation, ECs had a cobblestone morphology, the majority of actin filaments were localized around the periphery of cells, parallel with cell–cell junctions and no obvious gaps between cells (red staining as indicated in Fig. 4A). When ECs were exposed to HMGB1 (1000 ng/ml) for 12 h, the endothelial cell morphology changed, almost all cells were elongated with thick actin stress fibers that traversed the cells in the direction of cell elongation, F-actin reorganization,

and the increase in intercellular gaps (Fig. 4B). However, APS pretreatment inhibited F-actin reorganization in a concentration-dependent manner. Of which, only a small amount of intracellular stress fibers occurred when pretreated by APS (200 μg/ml) (Fig. 4C), further, APS (500 μg/ml) pretreatment did not occurred F-actin reorganization, endothelial F-actin was restored close to normal morphology (Fig. 4D).

3.5. Effects of APS pretreatment on HMGB1-induced morphology of endothelial tight junction protein ZO-1 and its protein expression

Paracellular permeability is controlled by tight junctions (TJs), which act as a permeability barrier to restrict the flow of fluid from the vascular lumen through the intercellular space (Martin, Harrison, Mason, & Jiang, 2011). Actin anchoring protein (ZO-1), as a membrane-associated protein, is the main ingredients of TJs, binds directly to F-actin (Eiselein, Wilson, Lamé, & Rutledge, 2007). Our study showed that ZO-1, located in the cells periphery, mostly formed a continuous line at cell–cell junctions, with occasional gaps (Fig. 5a-A). However, exposed to HMGB1 (1000 ng/ml) for 12 h, ZO-1 was still present at cell borders, but its distribution was much more fragmentary, indicating that tight junction integrity was disrupted (Fig. 5a-B). APS pretreatment could inhibit the diffuse redistribution of ZO-1 (Fig. 5a-C), particularly, APS pretreatment (500 μg/ml) significantly inhibited HMGB1-induced morphological changes of ZO-1 (Fig. 5a-D). Western blot analysis revealed that ZO-1 protein expressions were significantly reduced in HMGB1 treatment cells, compared with the control cells, indicating loss of ZO-1 from cell–cell junctions. APS pretreatment significantly inhibited the down-regulation of HMGB1-induced endothelial cells ZO-1 protein expressions (compared with the HMGB1-treated cells, $p < 0.01$, Fig. 5b). Based on the above results, it can be suggested that APS protected ECs against HMGB1-induced barrier dysfunction.

3.6. Suppression of APS pretreatment on HMGB1-induced RhoA expression in ECs

The actin cytoskeleton is an important regulator of the endothelial permeability barrier, as F-actin-disrupting agents have been shown to increase endothelial permeability (Gao et al., 2006; Guo et al., 2006; Kanthou et al., 2006). Rho regulates stress fiber formation in many cell types and is implicated in regulating endothelial permeability (Wojciak-Stothard & Ridley, 2002). As HMGB1 induced a progressive reorganization of stress fibers, we investigated whether Rho was activated by HMGB1 and inhibition effect of APS pretreatment on its activation. Our results showed that HMGB1 induced rapid activation of RhoA signaling pathway (compared with the control group, $p < 0.01$), RhoA was activated by HMGB1 at 15 min, but its activity returned to basal levels by 24 h, however, on the contrary, when cells were pretreated with APS (200 μg/ml and 500 μg/ml) for 24 h before HMGB1 (1000 ng/ml) exposure for 15 min, APS displayed marked inhibition on activation effect of HMGB1-induced RhoA signaling pathway, as shown in Fig. 6.

3.7. Inhibitive effects of APS pretreatment on HMGB1-induced pMLC expression in ECs

Phosphorylation of the regulatory subunit of myosin light chain (MLC) has been implicated in regulation of endothelial permeability after stimulation with thrombin, histamine, or inflammatory cytokines (Srinivas, Satpathy, Guo, & Anandan, 2006; Zeng et al., 2005). There is strong evidence that phosphorylated MLC activates myosin adenosine triphosphatase activity, leading to myosin filament assembly, cross-linking of filamentous actin, driving the

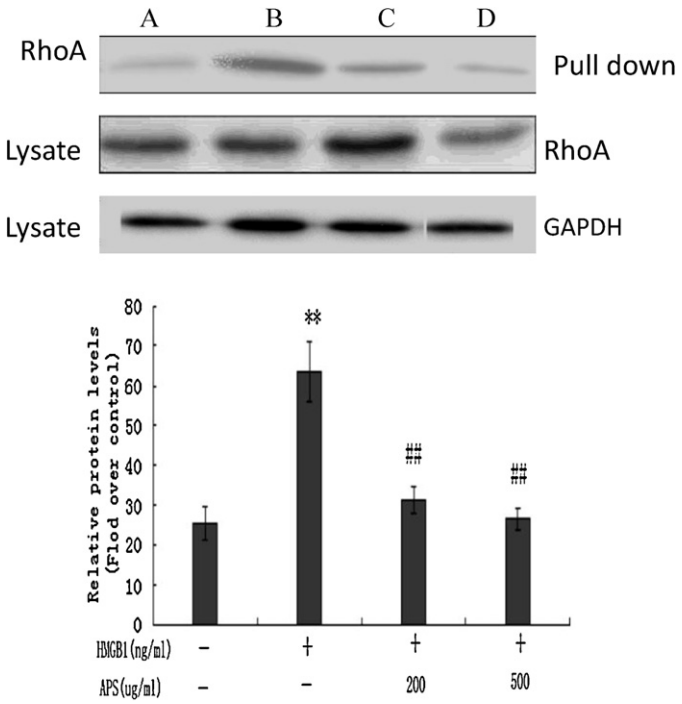

Fig. 6. Inhibitive effects of APS on HMGB1-induced RhoA expression in ECs. Cells were pretreated with APS for 24 h and then exposed to HMGB1 (1000 ng/ml) for 15 min. (A) Control group; (B) HMGB1 + 0 μg/ml APS group; (C) HMGB1 + 200 μg/ml APS group; (D) HMGB1 + 500 μg/ml APS group. Data were represented as mean ± SD ($n = 6$). $^{**}p < 0.01$ compared to the control group; $^{\#\#}p < 0.01$ compared to the HMGB1-treated group.

formation of actin stress fibers and generation of centripetal contractile force by the actomyosin apparatus (Ruiz-Loredo, López, & López-Colomé, 2011; van Nieuw Amerongen et al., 2007). Tensile forces, such as generated by phosphorylated myosin within actin stress fibers, are transmitted to membrane-bound tight junctions, which serve as actin anchors. These dynamic changes within the cytoskeleton lead to the development of spaces between cells and increased endothelial monolayer permeability to macromolecules and solutes (Bogatcheva, Adyshev, Mambetsariev, Moldobaeva, & Verin, 2007). Thus, MLC phosphorylation (pMLC) is a critical initiating event responsible for the enhanced paracellular flow of endothelial capillary leak (Srinivas et al., 2006). The mechanism of Rho regulating F-actin mainly lies in the activation of its downstream kinase-Rho kinase (ROCK), which can phosphorylate the myosin phosphatase target subunit (MYPT1/2), inhibit myosin phosphatase activity, also it can directly phosphorylate the MLC regulatory subunit, thus increases the levels of pMLC. Phosphorylated MLC drives myosin II interacting with F-acting, leading to increased contractility, as a result of increased permeability. Therefore, the inhibition of pMLC might be a critical step in suppressing HMGB1-induced the changes of morphology and increased permeability in ECs. We here, investigated whether APS pretreatment could inhibit HMGB1-induced pMLC in ECs. Results showed that HMGB1 stimulation (1000 ng/ml) for 30 min markedly increased the levels of pMLC (Fig. 7). However, APS pretreatment (200 and 500 μg/ml) for 24 h led to a significant down-regulation of pMLC proteins in ECs ($p < 0.05$ and $p < 0.01$ compared to the HMGB1-treated cells).

3.8. Roles of Rho/ROCK signaling pathways in HMGB1-induced endothelial permeability

It was proved that Rho/ROCK played a critical role in increase the levels of pMLC (Srinivas et al., 2006; Venkatesh et al., 2011).

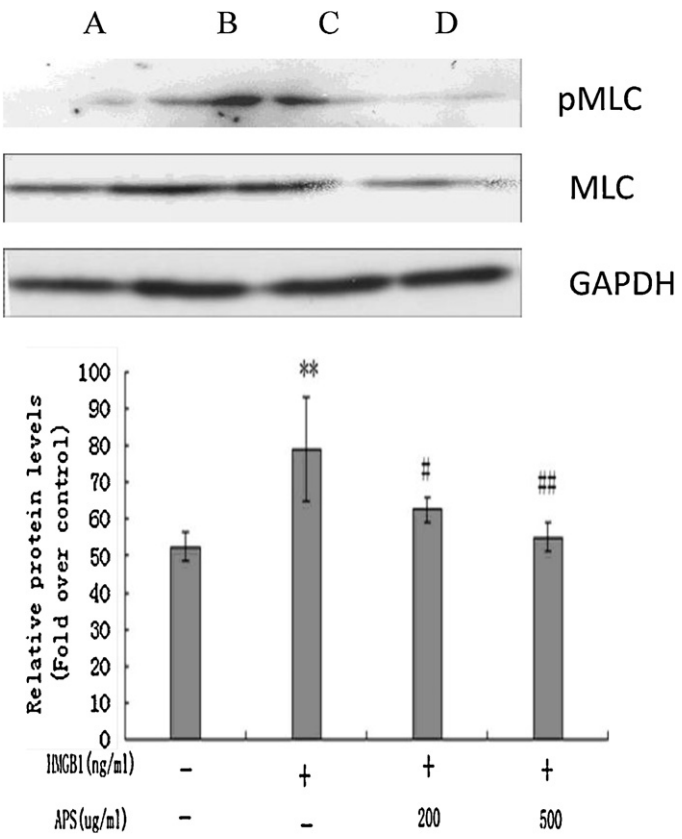

Fig. 7. Inhibitive effects of APS on HMGB1-induced pMLC expression in ECs. Cells were pretreated with APS for 24 h and then exposed to HMGB1 (1000 ng/ml) for 30 min. (A) Control group; (B) HMGB1 + 0 μg/ml APS group; (C) HMGB1 + 200 μg/ml APS group; (D) HMGB1 + 500 μg/ml APS group. Data were represented as mean ± SD ($n = 6$). $^{**}p < 0.01$ compared to the control group; $^{\#}p < 0.05$ and $^{\#\#}p < 0.01$ compared to the HMGB1-treated group.

Therefore, to confirm the roles of Rho/ROCK signaling pathways played in the endothelial hyperpermeability induced by HMGB1, the specific inhibitors were used in present study. As shown in Fig. 8, after ECs monolayers were exposed to HMGB1 (1000 ng/ml) for 8 h, where C3-transferase (Rho inhibitor, 15 μg/ml) or Y-27632 (ROCK inhibitor, 5 μM) were used, the inhibitors were added for the final 4 h of the 12 h HMGB1 incubation, the HMGB1-induced hyperpermeability in ECs were significantly inhibited ($p < 0.01$, compared to the HMGB1-treated cells), which implies that Rho/ROCK signaling pathways may be responsible for the suppressive effects of APS on HMGB1-induced increased permeability in ECs.

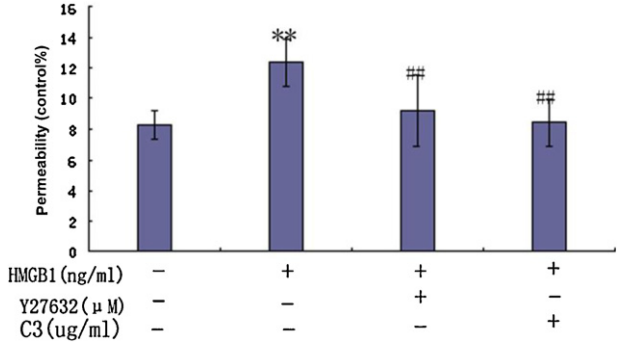

Fig. 8. Effects of Rho/ROCK pathways on HMGB1-induced endothelial permeability. Two specific inhibits, i.e. Y-27632 (5 μM) and C3 transferase (15 μg/ml), were added to the cells for the final 4 h of the 24 h HMGB1 (1000 ng/ml) exposured to cells. Data were presented as means ± SD ($n = 9$). $^{**}p < 0.01$ compared to the control group; $^{\#\#}p < 0.01$ compared to the HMGB1-treated group.

4. Conclusions

In this study, our findings indicated that APS suppressed HMGB1-induced a progressive increase in permeability and in stress fiber reorganization, cell elongation, and intercellular gap formation. The underlying molecular mechanisms may be that APS inhibited the HMGB1-induced increased permeability in ECs by blocking Rho/ROCK activation and subsequent pMLC.

Conflicts of interest

The authors have not disclosed any potential conflicts of interest.

Acknowledgements

We thank our teachers Xue Hua Chen, Jiang Fang Li, Bing Ya Liu and Zheng Gang Zhu at the Shanghai Institute of Digestive Surgery for their excellent technical assistance.

References

Bitto, A., Barone, M., David, A., Polito, F., Familiari, D., Monaco, F., et al. (2010). High mobility group box-1 expression correlates with poor outcome in lung injury patients. *Pharmacological Research: The Official Journal of the Italian Pharmacological Society*, *61*(2), 116–120.

Bogatcheva, N. V., Adyshev, D., Mambetsariev, B., Moldobaeva, N., & Verin, A. D. (2007). Involvement of microtubules, p38, and Rho kinases pathway in 2-methoxyestradiol-induced lung vascular barrier dysfunction. *American Journal of Physiology. Lung Cellular and Molecular Physiology*, *292*(2), L487–L499.

Cines, D. B., Pollak, E. S., Buck, C. A., Loscalzo, J., Zimmerman, G. A., McEver, R. P., et al. (1998). Endothelial cells in physiology and in the pathophysiology of vascular disorders. *Blood*, *91*(10), 3527–3561.

Downie, G. H., Ryan, U. S., Hayes, B. A., & Friedman, M. (1992). Interleukin-2 directly increases albumin permeability of bovine and human vascular endothelium in vitro. *American Journal of Respiratory Cell and Molecular Biology*, *7*(1), 58–65.

Eiselein, L., Wilson, D. W., Lame, M. W., & Rutledge, J. C. (2007). Lipolysis products from triglyceride-rich lipoproteins increase endothelial permeability, perturb zonula occludens-1 and F-actin, and induce apoptosis. *American Journal of Physiology. Heart and Circulatory Physiology*, *292*(6), H2745–H2753.

Fiuza, C., Bustin, M., Talwar, S., Tropea, M., Gerstenberger, E., Shelhamer, J. H., et al. (2003). Inflammation-promoting activity of HMGB1 on human microvascular endothelial cells. *Blood*, *101*(7), 2652–2660.

Gao, J., Zhao, W. X., Zhou, L. J., Zeng, B. X., Yao, S. L., Liu, D., et al. (2006). Protective effects of propofol on lipopolysaccharide-activated endothelial cell barrier dysfunction. *Inflammation Research: Official Journal of the European Histamine Research Society*, *55*(9), 385–392.

Guo, X. H., Huang, Q. B., Chen, B., Wang, S. Y., Li, Q., Zhu, Y. J., et al. (2006). Advanced glycation end products induce actin rearrangement and subsequent hyperpermeability of endothelial cells. *APMIS: Acta Pathologica, Microbiologica, et Immunologica Scandinavica*, *114*(12), 874–883.

Huston, J. M., Gallowitsch-Puerta, M., Ochani, M., Ochani, K., Yuan, R., Rosas-Ballina, M., et al. (2007). Transcutaneous vagus nerve stimulation reduces serum high mobility group box 1 levels and improves survival in murine sepsis. *Critical Care Medicine*, *35*(12), 2762–2768.

Kanthou, C., Kranjc, S., Sersa, G., Tozer, G., Zupanic, A., & Cemazar, M. (2006). The endothelial cytoskeleton as a target of electroporation-based therapies. *Molecular Cancer Therapeutics*, *5*(12), 3145–3152.

Karlsson, S., Pettila, V., Tenhunen, J., Laru-Sompa, R., Hynninen, M., & Ruokonen, E. (2008). HMGB1 as a predictor of organ dysfunction and outcome in patients with severe sepsis. *Intensive Care Medicine*, *34*(6), 1046–1053.

Lee, Y. S., Han, O. K., Park, C. W., Yang, C. H., Jeon, T. W., Yoo, W. K., et al. (2005). Pro-inflammatory cytokine gene expression and nitric oxide regulation of aqueous extracted Astragali radix in RAW 264.7 macrophage cells. *Journal of Ethnopharmacology*, *100*(3), 289–294.

Liu, D., Zhang, D., Scafidi, J., Wu, X., Cramer, C. C., & Davis. (2005). C1 inhibitor prevents Gram-negative bacterial lipopolysaccharide-induced vascular permeability. *Blood*, *105*(6), 2350–2355.

Liu, Q. Y., Yao, Y. M., Yu, Y., Dong, N., & Sheng, Z. Y. (2011). *Astragalus* polysaccharides attenuate postburn sepsis via inhibiting negative immunoregulation of CD4+ CD25(high) T cells. *PLoS One*, *6*(6), e19811.

Liu, Q. Y., Yao, Y. M., Zhang, S. W., & Sheng, Z. Y. (2011). Astragalus polysaccharides regulate T cell-mediated immunity via CD11c (high) CD45RB (low) DCs in vitro. *Journal of Ethnopharmacology*, *136*(3), 457–464.

Martin, T. A., Harrison, G. M., Mason, M. D., & Jiang, W. G. (2011). HAVcR-1 reduces the integrity of human endothelial tight junctions. *Anticancer Research*, *31*(2), 467–473.

Ren, X. D., & Schwartz, M. A. (2000). Determination of GTP loading on Rho. *Methods in Enzymology*, *325*, 264–272.

Ruiz-Loredo, A. Y., Lopez, E., & Lopez-Colome, A. M. (2011). Thrombin promotes actin stress fiber formation in RPE through Rho/ROCK-mediated MLC phosphorylation. *Journal of Cellular Physiology*, *226*(2), 414–423.

Shao, P., Zhao, L. H., Zhi-Chen, & Pan, J. P. (2006). Regulation on maturation and function of dendritic cells by *Astragalus mongholicus* polysaccharides. *International Immunopharmacology*, *6*(7), 1161–1166.

Shivanna, M., Rajashekhar, G., & Srinivas, S. P. (2010). Barrier dysfunction of the corneal endothelium in response to TNF-alpha: Role of p38 MAP kinase. *Investigative Ophthalmology & Visual Science*, *51*(3), 1575–1582.

Srinivas, S. P., Satpathy, M., Guo, Y., & Anandan, V. (2006). Histamine-induced phosphorylation of the regulatory light chain of myosin II disrupts the barrier integrity of corneal endothelial cells. *Investigative Ophthalmology & Visual Science*, *47*(9), 4011–4018.

van Nieuw Amerongen, G. P., Beckers, C. M., Achekar, I. D., Zeeman, S., Musters, R. J., & vanHinsbergh, V. W. (2007). Involvement of Rho kinase in endothelial barrier maintenance. *Arteriosclerosis, Thrombosis, and Vascular Biology*, *27*(11), 2332–2339.

Venkatesh, D., Fredette, N., Rostama, B., Tang, Y., Vary, C. P., Liaw, L., et al. (2011). RhoA-mediated signaling in Notch-induced senescence-like growth arrest and endothelial barrier dysfunction. *Arteriosclerosis, Thrombosis, and Vascular Biology*, *31*(4), 876–882.

Wang, H., Bloom, O., Zhang, M., Vishnubhakat, J. M., Ombrellino, M., Che, J., et al. (1999). HMG-1 as a late mediator of endotoxin lethality in mice. *Science*, *285*(5425), 248–251.

Wojciak-Stothard, B., & Ridley, A. J. (2002). Rho GTPases and the regulation of endothelial permeability. *Vascular Pharmacology*, *39*(4–5), 187–199.

Wolfson, R. K., Chiang, E. T., & Garcia, J. G. (2011). HMGB1 induces human lung endothelial cell cytoskeletal rearrangement and barrier disruption. *Microvascular Research*, *81*(2), 189–197.

Xiaolu, D., Jing, P., Fang, H., Lifen, Y., Liwen, W., Ciliu, Z., et al. (2011). Role of p115RhoGEF in lipopolysaccharide-induced mouse brain microvascular endothelial barrier dysfunction. *Brain Research*, *1387*, 1–7.

Yong, L., Yunxiao, S., Qiyan, X., Yu, Z., Jing, H., Mekoo, D. J., et al. (2010). Immunization with P277 induces vascular leak syndrome in C57BL/6 mice via endothelial damage. *Autoimmunity*, *43*(8), 654–663.

Yuan, Y., Sun, M., & Li, K. S. (2009). *Astragalus mongholicus* polysaccharide inhibits lipopolysaccharide-induced production of TNF-alpha and interleukin-8. *World Journal of Gastroenterology (WJG)*, *15*(29), 3676–3680.

Zeng, L., Xu, H., Chew, T. L., Eng, E., Sadeghi, M. M., Adler, S., et al. (2005). HMG CoA reductase inhibition modulates VEGF-induced endothelial cell hyperpermeability by preventing RhoA activation and myosin regulatory light chain phosphorylation. *The FASEB Journal: Official Publication of the Federation of American Societies for Experimental Biology*, *19*(13), 1845–1847.